Discover Applied Sciences

Research

Innovative smart colorimetric sensor for nitrite detection in poultry packaging

Sreedevi Paramparambath[1,2] · Mithra Geetha[1] · Abdulrhman Mohammed Alahzm[1] · Maryam Al-Ejji[1] · Kishor Kumar Sadasivuni[1,2]

Received: 24 March 2024 / Accepted: 8 May 2024
Published online: 13 May 2024

Abstract
Detecting nitrite ions is crucial for environmental and health monitoring, given the prevalence of nitrites in water sources and meat. Colorimetric methods provide a cost-effective, rapid, and straightforward means of nitrite ion detection. This study focuses on monitoring nitrite levels in meat to ensure its safe consumption. Three different dyes—Bromophenol blue (B.P.B.), Eriochrome Black T (E.B.T.), and Potassium permanganate (KMnO4)—were employed to identify and quantify nitrite ions under various experimental conditions such as variable pH, temperature, concentration, and selectivity. UV–visible studies revealed low average detection limits of 0.2054 mM for E.B.T. dye, 0.218 mM for B.P.B., and 3.317 mM for $KMnO_4$ dye solution. An Internet of Things (IoT)-based, portable, and cost-effective device for colorimetric nitrite ion detection was also developed. This innovative system integrates a connected detection mechanism within a smart device, enabling swift acquisition of red, green, and blue (RGB) readings for real-time applications in nitrite ion detection. This development has the potential to offer an economical, precise, and easily transportable method for monitoring nitrite ions, presenting a promising approach to creating accessible tools in this field.

Article Highlights

- This study focuses on the colorimetric detection for monitoring nitrite ions in meat.
- A three-dye system was utilized for identifying and quantifying nitrite ions and its efficacy were tested under various experimental conditions.
- An innovative IoT based device was developed for the detection of nitrite ion using colorimetry.

Keywords Sodium nitrite · Meat curing · Colorimetry · Sensor · Ions

Supplementary Information The online version contains supplementary material available at https://doi.org/10.1007/s42452-024-05943-w.

✉ Kishor Kumar Sadasivuni, kishor_kumars@yahoo.com | [1]Centre for Advanced Materials, Qatar University, P. O. Box 2713, Doha, Qatar. [2]Department of Mechanical and Industrial Engineering, Qatar University, P. O. Box 2713, Doha, Qatar.

1 Introduction

Meat curing is an ancient practice which allows people to increase the shelf life of meat by improving its texture and taste. This primitive technique involves the addition of nitrites, salt, and other seasonings to convert meat into cured products such as ham, salami, bacon, etc. In modern society, processed food has gained much more attention than home-cooked dishes as it is easy to cook and saves time [1, 2]. The nitrate ion (NO_3^-) was initially discovered, followed by the nitrite ion (NO_2^-) due to the advancement of research [3]. Nitrite and nitrate salts are similar to sodium and potassium, considered typical food preservatives used in meat processing. However, in 1960 the invention of N-nitroso compounds increased the safety concerns of using nitrate and nitrite in meat processing. Nitrates and nitrites are frequently observed and studied due to their toxicity.

Sodium nitrate is added to meat to enhance and stabilize the red color in meat such as bacon, hot dogs, etc. Initially, sodium nitrate is added to the dry meat and slowly converts into nitrite. The International Food Information Council Foundation provides an example of consumer's conflicting relationship between humans and food preservatives through the Food and Health survey conducted in the year 2015 [4]. Despite their long history of being employed for food preservation, nitrate and nitrite faced a potential ban from food applications in the 1970s due to emerging data indicating potential health risks [5]. Still, nitrite remains the most feared compound among the food additives by consumers [6]. The implementation of sodium nitrite in the poultry industry has been quite debatable due to its possible health risks.

Sodium nitrite inhibits the germination of Clostridium botulinum species and can impart a pink color to the meat as it reacts with the myoglobin of the meat [7]. The pink coloration is due to the conversion of myoglobin to bright red nitroso myoglobin, and, on heating, it converts into pink-colored nitrosohemochrome. The toxicological implication of nitrite is due to the formation of highly carcinogenic nitroso compounds [8, 9] and peroxinitrite [10, 11]. This compound induces carcinogenicity in living beings. Nitrosamines, a carcinogen, are generated in meat when nitrites are added to it. The World Health Organization (WHO) recommends that taking 50 g of processed meat per day raises the risk of developing bowel cancer by 18%.

Many methods are utilized for identifying nitrites and nitrites, such as ion chromatography [12–15], fluorescence [16], electrochemistry [17–20], chemiluminescence [21] and capillary electrophoresis [22]. Nevertheless, these techniques are time-consuming and require workforce and expensive instrumentation. Colorimetric analysis using Greiss assay is an alternative that allows portable, low cost and rapid detection [23, 24]. Colorimetric analysis for Nitrite detection enables regular poultry nitrite content monitoring. Monitoring the nitrite level in meat enhances the quality of food intake, improving the quality of life. It aids in continuously advancing research and monitoring initiatives, which play a crucial role in preserving the optimal mineral equilibrium and boosting the well-being and productivity of poultry populations. This research introduces a unified colorimetric detection technique alongside a streamlined procedure.

2 Materials and methods

2.1 Materials required

Bromophenol Blue (BPB), Eriochrome Black T (EBT), Potassium Permanganate ($KMnO_4$), Sodium Hydroxide (NaOH), and Hydrochloric Acid (HCl) were all obtained from Sigma-Aldrich. Analytical-grade chemicals were used in the study. The purified water for the experiment was obtained from the Milli pore Milli Q water system. The instrument Biochrom UV–Visible spectrophotometer is utilized for UV–vis characterization with a scanning range from 190 to 1100 nm. The dye samples are scanned from 300 to 800 nm at a medium speed.

2.2 Dye preparation, characterization and optimization of kinetic parameters

The solutions of $KMnO_4$, Bromophenol Blue and Eriochrom Black T. were prepared at a concentration of 0.003 M and utilized consistently throughout the experiment. The impact of pH on various test substances was examined using acidic (at pH 2, 4, 6), neutral, and basic (at pH 9, 12) solutions in combination with the different dye solutions. Each dye solution (10 mL) was individually mixed with 1 mL of 0.5 ppm test solution (a mixture of ethanol, formic acid, and methanol) at adjusted pH levels. Alterations in color and the time taken for corresponding changes were observed.

The impact of concentration and temperature on these test solutions concerning selected dyes was explored, focusing on visible color changes at specific pH levels, which varied among the different dyes. The detection threshold of the dyes was monitored across test solution concentrations ranging from 0.05 to 15 ppm, while the temperature effects were studied at 25 °C, 50 °C, 75 °C, and 100 °C.

The experiments were conducted using solutions containing 2 ppm of Bromophenol Blue (B.P.B.), and a combination of B.P.B. with Eriochrome Black T. UV spectrophotometry was utilized for the characterizations at room temperature. After the characterizations and data analysis, an absorbance–wavelength graph was generated.

2.3 Development of a smartphone-assisted sensor prototype

The fabrication of an IOT-based colorimetric sensor prototype is very simple and cost-effective. The sensor prototype is shown in Fig. 1. The colorimetric instrument is divided into three parts, the light source, the sample area, and the color detector area. Light Emitting Diode (LED)s were utilized as the illumination source, featuring four distinct colors: red, blue, white, and green. Subsequently, two compartments are designated for the sample area after the region where the light is emitted. A protective case created via 3D printing covers the sample area, immediately succeeded by a detection zone fitted with a color sensor. To ensure consistent results, the light source, sample area, and sensor are aligned horizontally, and the prototype is painted black to minimize any reflections. Two containers, each containing dye solutions, are arranged sequentially, one after the other, and are exposed to the L.E.D. light source. The color sensor then captures the light transmitted from the sample area. By analyzing this transmitted light, the sensor establishes the RGB values. When biomarkers are introduced, the dye solution experiences a color change. Through the sensor prototype's connection to a device (LCD/smartphone) via Bluetooth, the sensor identifies alterations in the dye solutions' colors and exhibits distinct RGB values.

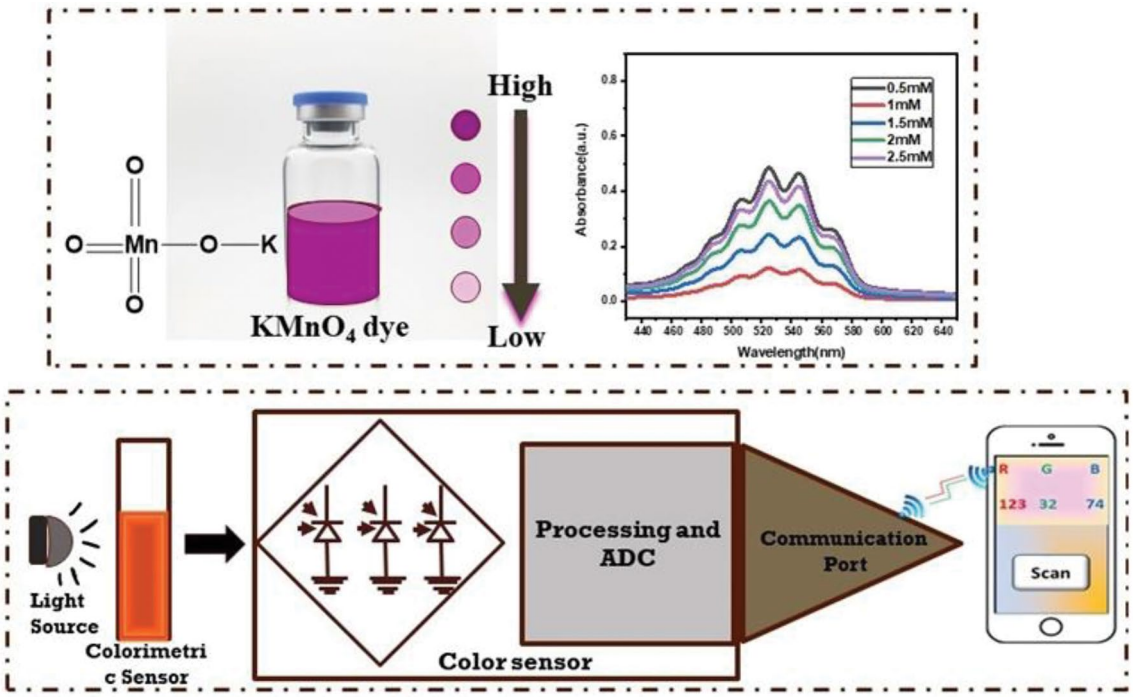

Fig. 1 Pictorial representation of adopted technique for Nitrite detection

3 Results and discussion

To develop an exceptionally sensitive colorimetric sensor for NO_2^- ions, we introduced $NaNO_2$ at a concentration of 0.5 mM into dye solutions within acidic, basic, and neutral environments, and then closely observed for any noticeable color change. Moreover, the dye's pH effect, concentration effect, temperature effect, response time and selectivity were examined and evaluated.

3.1 pH effect and response time

The pH of the dye solution varies with pH values 3, 5, 7, 9 and 12, and the pH effect of the sodium nitrite solution is studied in different dyes. Furthermore, the response time of the dye solution concerning the test solution was also examined. Data were assessed before and after introducing the test solutions to the dyes across a range of pH levels for each dye.

When examining Bromophenol blue dye, a noticeable color transformation occurs at pH 3, where the yellow hue turns colorless upon adding $NaNO_2$. This visible color alteration takes place within 3 s. Figure 2A illustrates the color shift of B.P.B. at pH 3 when introducing 0.5 M NaNO2 into the solution. Initially, the peak for B.P.B. appears at 593.3 nm with an absorbance of 0.03 a.u. Subsequently, upon adding $NaNO_2$ to the dye solution, a peak shift to 589.2 nm with a higher absorbance of 0.32 a.u. is observed. In the Eriochrome Black T (E.B.T.) dye, the wavelength and absorbance for the undisturbed dye solution are noted at 523.5 nm and 0.034 a.u., respectively. A visible color alteration from pink to colorless is observed at pH 3 upon adding 0.5 mM of $NaNO_2$. This is shown in Fig. 2B. Upon introducing the analyte solution,

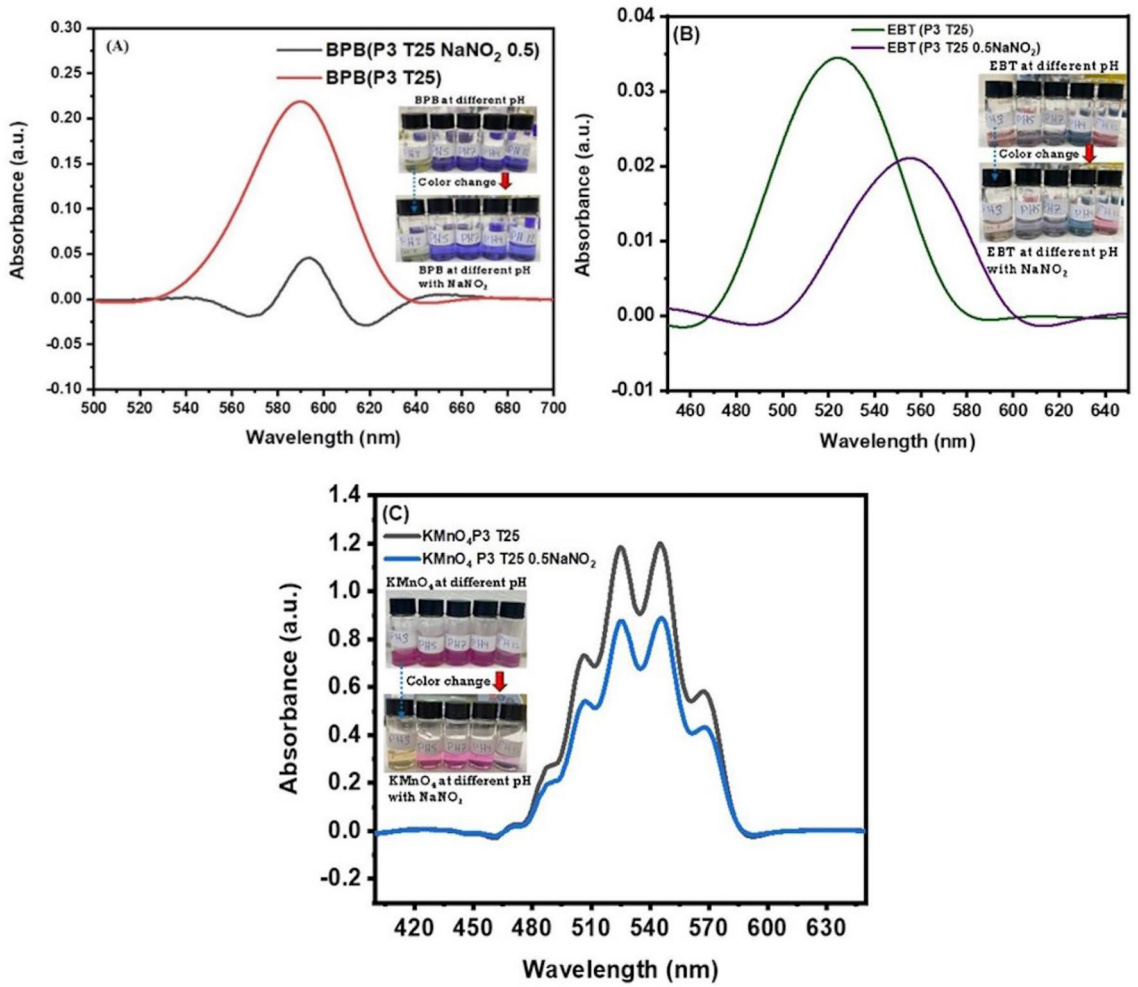

Fig. 2 Shows the pH effect and color change in dyes, **A** BPB, **B** EBT and **C** $KMnO_4$ while adding 0.5 mM $NaNO_2$

the wavelength shifts to 555.6 nm with a decreased absorbance of 0.021 a.u. For both E.B.T. and B.P.B., the color change with lower absorbance may be attributed to the chelate ligand formation in the dye due to its interaction with nitrite ions in the analyte solution.

When $KMnO_4$ is analyzed, the bare dye solution shows pink color in all different pH. Figure 2C shows the pH effect of $KMnO_4$. At pH 3, when $NaNO_2$ is added to the dye the pink changes to colorless with a decrease in absorbance. This occurrence is typical in cases of strongly conjugated systems. Nevertheless, it frequently relies on the solvent used and could result from electronic transitions between various vibrational energy levels available for each electronic state [25].

3.2 Temperature effect

When fluctuations occur in the temperature of the surrounding environment, any biosensor must maintain the stability of its detection system. The stability of the dye system and the physical dimensions of the molecules are both influenced by changes in temperature. From a thermodynamic perspective, an increase in vapor pressure leads to a corresponding temperature rise, reducing sensitivity and responsiveness. Therefore, minimizing the impact of temperature is essential to ensure an effective sensing system. To investigate the effect of temperature, the dye solutions were heated at 25, 50, 75 and 90 °C, and $NaNO_2$ (0.5 mM) was added to the dye solutions. From the results, it is evident that the dye solutions are independent of the temperature changes. Figure 3A, B and C shows the temperature effects of BPB, EBT and KMnO4 dye solutions with 0.5 mM of $NaNO_2$ respectively.

3.3 Sensitivity study

To examine the sensitivity of the dye solution, different concentrations of $NaNO_2$ range from 0.5 mM to 2.5 mM. The concentration effect is studied at room temperature. The aim was to examine the impact of $NaNO_2$ concentration on dye behavior, particularly concerning alterations in color. This examination was depicted and studied in Fig. 4. A fundamental principle directing this research is the Beer-Lambert law, which elucidates a direct correlation between a solution's absorbance and its concentration. As per this law, A represents the absorption of the solution, ε (epsilon) stands for the molar absorptivity or molar extinction coefficient of the substance, b signifies the path length (typically the width of the container holding the solution), and C denotes the concentration of the substance within the solution and is linked by the equation:

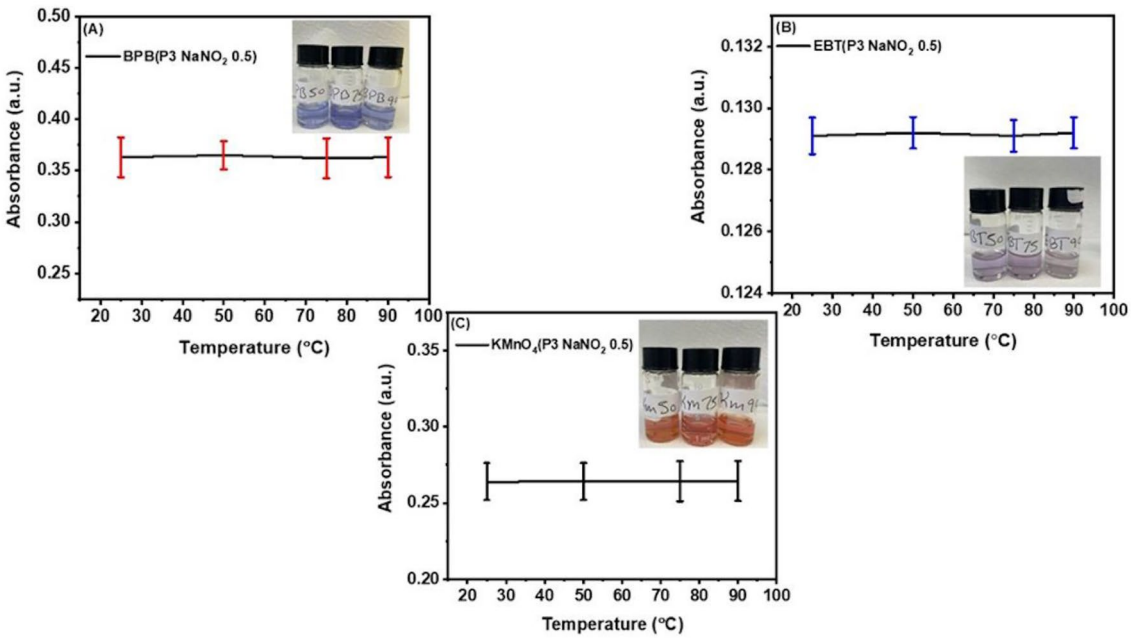

Fig. 3 Shows the temperature effect of dye solutions at various temperatures such as 25,50,75 and 90 °C. **A** Absorbance and color change graph of B.P.B. dye solution, **B** absorbance and color change graph of E.B.T. dye and **C** absorbance and color change graph of KMnO4 solution

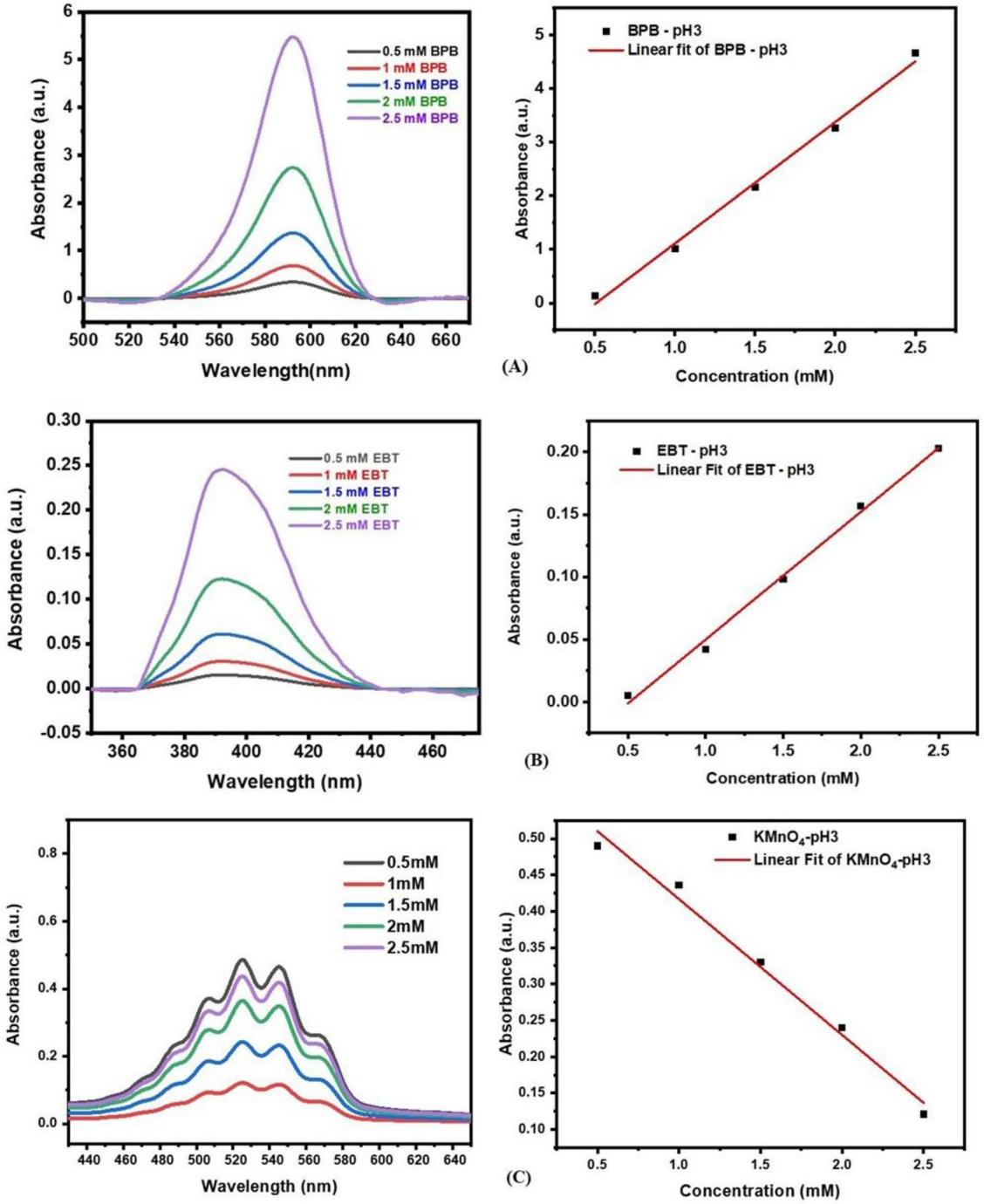

Fig. 4 Graphical representation of $NaNO_2$ sensitivity towards dye solution. U.V. absorption and calibration plot of **A** B.P.B., **B** E.B.T. and **C** $KMnO_4$ with respect to nitrite ion concentration ranging from 0.5 – 2.5 mM

$$A = \in . b. C \tag{1}$$

The principle essentially asserts that the absorbance of a solution is directly connected to both its concentration and the path length. The absorbance was assessed for each $NaNO_2$ concentration applied to the dye solutions in the experiment. The correlation between absorbance and concentration was graphed, resulting in a linear calibration curve, as depicted in Fig. 4. This curve enables the estimation of concentration based on absorbance readings, presenting

a valuable tool for subsequent analyses and practical use. An important observation from the experimental findings was that color transformation occurred more swiftly in the dye solutions when higher concentrations of $NaNO_2$ were employed. This indicates that the concentration of $NaNO_2$ notably influences the speed or degree of color modification in the dye solutions, signifying a potentially crucial facet for further exploration and real-world applications.

In this investigation, the Limit of Detection (L.O.D.) was established as a crucial analytical parameter, determining the minimum concentration of $NaNO_2$ analyte reliably detectable within a sample. Using the formula 3σ/m, where m represents the slope of the calibration plot, and σ indicates the standard deviation of the intercept, utilized for L.O.D. calculation. The highest absorbance point of the dye was employed in creating the calibration curve, and Fig. 4 illustrates this specific calibration curve for $NaNO_2$. The calibration curve equation is $y = mx + c$, with y representing absorbance, x as the analyte concentration, m denoting the slope, and c indicating the intercept. For further applications this curve enables concentration related to absorbance measurements. The remarkable observations from the experimental analysis where rapid color change was observed for higher concentration of $NaNO_2$ was added to the dye solution. This area indicates the potential aspect of further studies and application as concentration of $NaNO_2$ has significant impact in the rate of color change of the dye solution. Figure 4A, B, and C represent the concentration effect and limit of detection of BPB, EBT and $KMnO_4$ dyes respectively.

For B.P.B. dye, from the calibration curve, the L.O.D. value calculated using the formula were obtained as 0.2 mM with R^2 value 0.9942. Similarly, for E.B.T. dye the value obtained for L.O.D. was 0.2 mM with an R^2 value of 0.9949. For the dye $KMnO_4$ the L.O.D. value determined was 3.3 mM with R^2 value 0.986. The L.O.D. value is crucial data as it indicates the sensitivity of the sensor. Low L.O.D. value specifies the capability of the sensor for determining lower concentration of analyte ion. The L.O.D. values obtained for these dye solutions are key indicators for further experimental and analytical applications.

3.4 Selectivity study

To establish the selectivity of the sensor further studies with various ions were carried out in the dye solution such as Sodium chloride (NaCl), sodium Bromide (NaBr), Sodium acetate (CH_3COONa), sodium dihydrogen phosphate (NaH_2PO_4). For the UV–Visible analysis the test solution was taken at a concentration of 0.5 mM in the dye solutions. From the studies it is evident that all three dye solutions are selective towards nitrite ion. Moreover, the nitrite ion selectivity was measured using the formula:

$$\Delta\lambda = \frac{\lambda_x - \lambda_0}{\lambda_0} \times 10 \tag{2}$$

This equation is the calculation of relative wavelength change from UV–Visible analysis. λ_x is the wavelength obtained from UV analysis after addition of the analyte and λ_0 is the wavelength obtained from neat dye solution. Figure 5 shows the selectivity analysis of dye solutions at pH 3. From the analysis it is evident that there is no effect of interfering ions on the dye solutions. Figure 5A represents BPB dye, 5B represents EBT dye solution and 5C represents $KMnO_4$ dye solution.

3.5 Sensor prototype for real time analysis and quantification of nitrite ions

In order to identify and determine the nitrite ion concentration, a portable and user-friendly sensor is developed. The prototype designed was utilized for identifying the nitrite ions using a three-dye system as shown in Fig. 6 along with the schematic representation of real time analysis using a three-dye system. Figure 6B is the representation of sensor prototype's upper view. And 6C is the representation of real time three dye system.

Utilizing this three-dye system has proven to be a precise and reliable method for real time detection of nitrite ions. By using the three dyes as sensing components and referring to the RGB chart, it was possible to effectively identify nitrite ions. The sensor prototype exhibited distinct RGB values when exposed to 0.5 mM, 1.5 mM and 2.5 mM nitrite ions using different dye combinations, as tabulated in Table 1. This study illustrated the potential of generating unique RGB charts for various nitrite ion concentrations, with each specific RGB value corresponding to a particular nitrite ion concentration. This association could then be utilized to quantify nitrite ions in the test sample. The analytical method proposed in this research, employing the developed device, provides an accurate and reliable means of rapidly detecting nitrite ions on-site, particularly in water and poultry feed. Furthermore, this technique may have applications in monitoring nitrite ions in various fields.

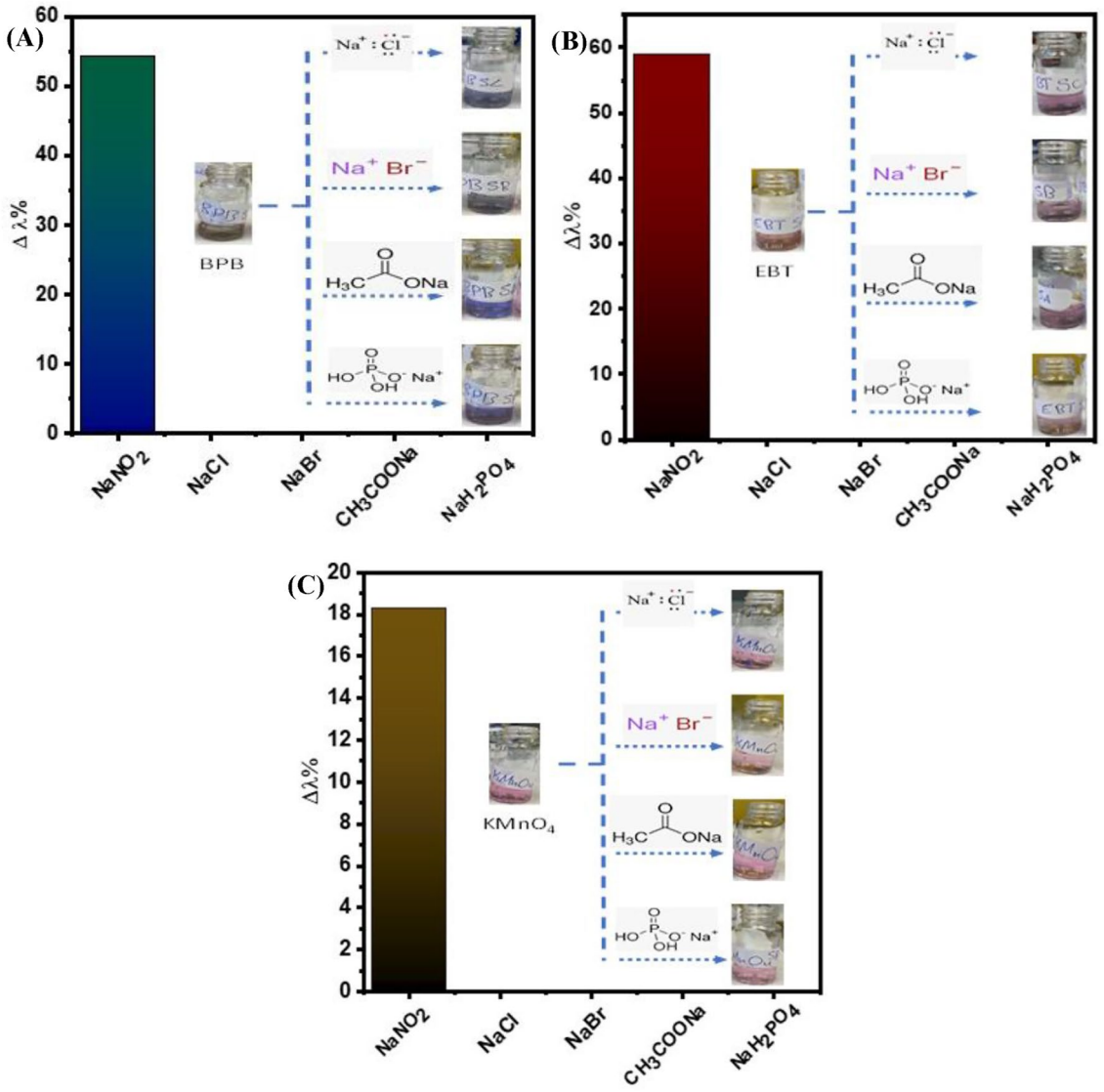

Fig. 5 Selectivity analysis of Nitrite ion in **A** B.P.B. dye solution, **B** E.B.T. dye and **C** $KMnO_4$ dye solution

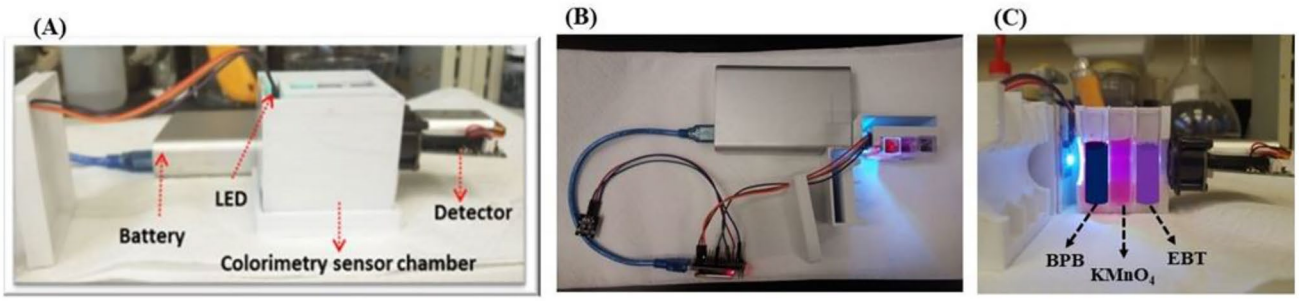

Fig. 6 Shows the pictorial representation of the fabricated sensor prototype using a three-dye system. **A** the components of the fabricated sensor, **B** Upper view of the sensor prototype and **C** the three-dye system in real time analysis

Table 1 RGB value chart for 0.5 mM, 1.5 mM and 2.5 mM nitrite ions in different Configurations of dye set

Dye combinations				RGB values
Concentration	$KMnO_4$	EBT	BPB	
0.5 mM	0	0	0	130,110,50
	NO_2–	0	0	55,61,108
	0	NO_2–	0	58,99,95
	NO_2–	NO_2–	0	65,101,124
	0	0	NO_2–	75,18,38
	NO_2–	0	NO_2–	81,110,79
	0	NO_2–	NO_2–	94,110,61
	NO_2–	NO_2–	NO_2–	110,90,86
1.5 mM	0	0	0	183,161,103
	NO_2–	0	0	110,114,160
	0	NO_2–	0	111,150,148
	NO_2–	NO_2–	0	115,154,177
	0	0	NO_2–	128,71,92
	NO_2–	0	NO_2–	133,164,132
	0	NO_2–	NO_2–	147,163,110
	NO_2–	NO_2–	NO_2–	163,140,140
2.5 mM	0	0	0	211,190,131
	NO_2–	0	0	136,142,190
	0	NO_2–	0	140,181,176
	NO_2–	NO_2–	0	146,182,202
	0	0	NO_2–	155,100,121
	NO_2–	0	NO_2–	162,191,160
	0	NO_2–	NO_2–	177,191,140
	NO_2–	NO_2–	NO_2–	191,173,167

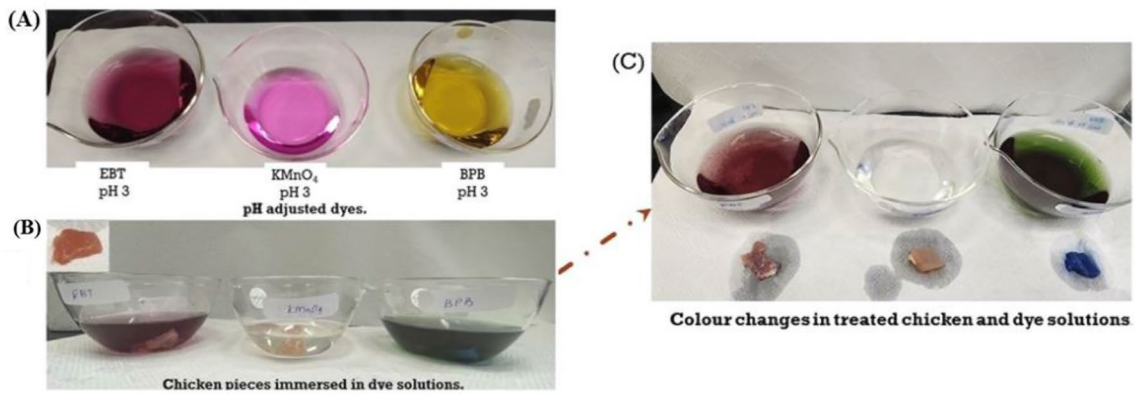

Fig. 7 Practical application of Nitrite detection in chicken. **A** Dye solutions of EBT, KMnO4 and BPB at pH 3, **B** pictorial representation of dye solutions with chicken pieces. (Insight is the photo of bare chicken piece) and **C** the color change of dye solutions and chicken due to the presence of nitrite

3.6 Practical applications

To assess the real-time application of our method, we conducted a colorimetric experiment. Chicken breasts are immersed in a solution containing 0.5 M $NaNO_2$ for about 2 days and then subjected to analysis. We prepared dye solutions with a pH of 3, and dipped 10 g chicken pieces into this pH adjusted solution. We observed the color change of the dye solution upon interaction with $NaNO_2$ infused chicken breasts, these finds are represented in Fig. 7. In

Fig. 7a, the depiction of pH adjusted dye solutions including EBT, $KMnO_4$ and BPB, while Fig. 7b depicts these chicken pieces immersed in them. It is remarkable that the presence of nitrite containing chicken altered the color of the dye solution and the chicken itself, as shown in Fig. 7c. Furthermore, a supplementary video containing the above-mentioned analysis has been included.

4 Conclusion

This research lays the groundwork for creating a highly sensitive and selective IoT-based sensor designed for swift and real-time detection of sodium nitrite ions in packed meat. The study utilized E.B.T., B.P.B., and $KMnO_4$ dyes, proving successful in detecting nitrite ions. UV studies and calibration graphs revealed impressively low average detection limits: 0.2 mM for E.B.T. dye, 0.2 mM for B.P.B., and 3.3 mM for $KMnO_4$ dye solution. The stability of these dyes was examined across varying temperatures, demonstrating consistent performance. The crucial sensitivity and selectivity of these colorimetric assays make them suitable for on-site testing and continuous monitoring. Additionally, the dyes exhibited exceptional selectivity even in the presence of other interfering molecules. The effectiveness of the detection process was validated through the creation of a 3D-printed prototype device. By combining the 3D-printed prototype with RGB analysis, the research team achieved the measurement and identification of nitrite ions, represented visually through a distinctive RGB chart. This technological advancement holds significant importance in the realm of nitrite detection, showcasing its potential applications in environmental and health assessments.

Author contributions Sreedevi Paramparambath Investigation and Writing- Original draft preparation Mithra Geetha: Data curation and Visualization. Abdulrhman Mohammed Alahzm: Investigation. Maryam Al-Ejji: Reviewing and Editing. Kishor Kumar Sadasivuni: Methodology, Supervision, Funding acquisition and Validation.

Funding This work was supported by the Qatar National Research Fund under Grant No. MME03-1226-210042 and NPRP14S-0317-210064. The statements made herein are solely the responsibility of the authors.

Data availability The data from this study will be made available on request.

Code availability Not applicable.

Declarations

Ethics approval and consent to participate Not applicable. All the authors participated in the research and analysis.

Consent for publication All the authors approved communicating this manuscript for publication.

Competing interests The authors hereby declare no known conflicting interests that influenced this research and manuscript.

References

1. Torstensson L, Johansson R, Mark-Herbert C. Food dishes for sustainable development: a Swedish food retail perspective. Foods. 2021;10(5):932.
2. Yu N, et al. Combined sterilizing effects of nano-ZnO and ultraviolet on convenient vegetable dishes. LWT-Food Sci Technol. 2015;61(2):638–43.
3. Bedale W, Sindelar JJ, Milkowski AL. Dietary nitrate and nitrite: benefits, risks, and evolving perceptions. Meat Sci. 2016;120:85–92.
4. Foundation. IFIC. 2009 food and health survey: Consumer attitudes toward food, nutrition, and health. International Food Information Council. 2007.
5. Cassens RG, Cassens R. Nitrite-cured meat: a food safety issue in perspective. Trumbull CT: Food & Nutrition Press; 1990.

6. Downs M. The Truth About 7 Common Food Additives. WebMD. Diakses dari www. webmd. com/.../the-truth-about-sevencommon-food-additives. 2008.
7. Sebranek JG. Basic curing ingredients. Ingredients in meat products: properties, functionality and applications. New York: Springer, New York; 2009.
8. Karwowska M, Kononiuk A. Nitrates/nitrites in food—risk for nitrosative stress and benefits. Antioxidants. 2020;9(3):241.
9. Stoica M. Overview of sodium nitrite as a multifunctional meat-curing ingredient. The Annals of the University Dunarea de Jos of Galati. Fascicle VI-Food Technol. 2019;43(1):155–67.
10. Breen C, et al. Time-resolved luminescence detection of peroxynitrite using a reactivity-based lanthanide probe. Chem Sci. 2020;11(12):3164–70.
11. Ferrer-Sueta G, et al. Biochemistry of peroxynitrite and protein tyrosine nitration. Chem Rev. 2018;118(3):1338–408.
12. Li H, Meininger CJ, Wu G. Rapid determination of nitrite by reversed-phase high-performance liquid chromatography with fluorescence detection. J Chromatogr B Biomed Sci Appl. 2000;746(2):199–207.
13. Tsikas D. Analysis of nitrite and nitrate in biological fluids by assays based on the Griess reaction: appraisal of the Griess reaction in the L-arginine/nitric oxide area of research. J Chromatogr B. 2007;851(1–2):51–70.
14. Berardi G, et al. Different use of nitrite and nitrate in meats: a survey on typical and commercial Italian products as a contribution to risk assessment. Lwt. 2021;150:112004.
15. Coviello D, et al. Validation of an analytical method for nitrite and nitrate determination in meat foods for infants by ion chromatography with conductivity detection. Foods. 2020;9(9):1238.
16. Gao F, et al. Ultrasensitive and selective determination of trace amounts of nitrite ion with a novel fluorescence probe mono [6-N (2-carboxy-phenyl)]-β-cyclodextrin. Anal Chim Acta. 2005;533(1):25–9.
17. Miao P, et al. Functionalization of platinum nanoparticles for electrochemical detection of nitrite. Anal Bioanal Chem. 2011;399:2407–11.
18. Gholivand M-B, Jalalvand AR, Goicoechea HC. Computer-assisted electrochemical fabrication of a highly selective and sensitive amperometric nitrite sensor based on surface decoration of electrochemically reduced graphene oxide nanosheets with CoNi bimetallic alloy nanoparticles. Mater Sci Eng C. 2014;40:109–20.
19. Dutt J, Davis J. Current strategies in nitrite detection and their application to field analysis. J Environ Monit. 2002;4(3):465–71.
20. Dorovskikh SI, et al. Electrochemical sensor based on iron (II) phthalocyanine and gold nanoparticles for nitrite detection in meat products. Sensors. 2022;22(15):5780.
21. Adarsh N, Shanmugasundaram M, Ramaiah D. Efficient reaction based colorimetric probe for sensitive detection, quantification, and on-site analysis of nitrite ions in natural water resources. Anal Chem. 2013;85(21):10008–12.
22. Lee KS, et al. Electrophoretic analysis of food dyes using a miniaturized microfluidic system. Electrophoresis. 2008;29(9):1910–7.
23. Sieben VJ, et al. Microfluidic colourimetric chemical analysis system: application to nitrite detection. Anal Methods. 2010;2(5):484–91.
24. Sun J, et al. Measurement of nitric oxide production in biological systems by using Griess reaction assay. Sensors. 2003;3(8):276–84.
25. Matsukawa Y, Umemura K. Detection of redox properties of (6, 5)-enriched single-walled carbon nanotubes using potassium permanganate (KMnO4). C. 2020;6(2):30.